Development of Ground-Based Microwave Radiometer Network and Monitoring System using 1-Dimentional Variational Technique

Kentaro Araki[1], Hiromu Seko[1], Hiroshi Ishimoto[1], Takuya Tajiri[1], Koichi Yoshimoto[2,1], Makoto Matsumoto[2], Tomohiro Takeda[2], Yoshiyuki Kawano[2], Kenji Suzuki[2], Kazumasa Nakayama[2]

1: Meteorological Research Institute, Tsukuba, Ibaraki, Japan

2: Japan Meteorological Agency, Minato-ku, Tokyo, Japan

e-mail: araki@mri-jma.go.jp

1. Introduction

In Japan, landslides and flash floods are often caused by quasi-stationary convective bands (QSCBs) during the rainy season, and many previous studies have pointed out the importance of large amounts of water vapor supply in the lower atmosphere in the formation of QSCBs. Therefore, the Japan Meteorological Agency (JMA) has been enhancing water vapor observations in order to improve the monitoring and forecasting techniques for QSCBs and to elucidate the mechanism of QSCBs. As part of this effort, we have established a network of ground-based microwave radiometers (MWRs) in FY2022 and developed a system for real-time monitoring using data assimilation methods. In this report, we describe the outline of the MWR observation network and monitoring system, the verification results of vertical profiles of air temperature and water vapor density, and the initial observation results including precipitation cases.

2. Microwave radiometer network

First, RPG-HATPRO-G5 was adopted for this MWR observation network. This MWR observes brightness temperature at intervals of 1 second to several minutes with 7 channels in the 22 to 31 GHz band sensitive to water vapor and cloud water, and 7 channels in the 51 to 58 GHz band sensitive to oxygen. Based on this data, vertical profiles of temperature and water vapor density can be estimated using neural networks (NNs) and data assimilation methods developed at the Meteorological Research Institute (MRI).

We have installed MWRs at 17 stations, mainly in western Japan where heavy rainfall due to QSCBs and typhoons is likely to occur. An overview of the stations and the MWR observation network are shown in Figs. 1 and 2. Observation sites were chosen where the JMA had already installed wind profilers. This allows us to obtain atmospheric thermodynamic profiles of air temperature and water vapor density and dynamic profiles of wind at the same time.

Figure 1. Overview of MWR station at Owase. The equipment in the foreground is MWR and the one in the background is WPR.

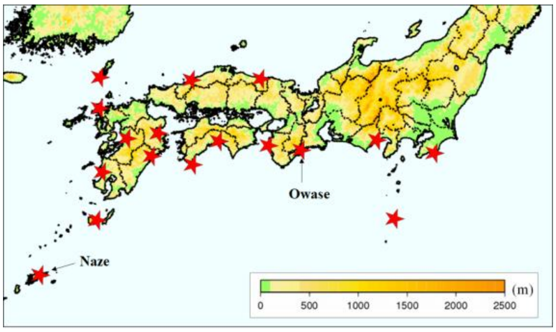

Figure 2. MWR Observation Network. Red stars mean MWR observation points. Paint color indicates elevation (m).

3. Monitoring system using 1DVAR technique

The NN has been widely used as a retrieval method for temperature and water vapor density using MWR data. On the other hand, it has been pointed out that NN has large errors, especially in the upper atmosphere. Therefore, our group at the MRI have developed a vertical one-dimensional variational data assimilation method (1DVAR) that combines numerical weather model results with MWR data and verified that its accuracy is better than that of NN and model results (Araki et al., 2015).

In this study, a new 1DVAR method was developed at JMA based on MRI's 1DVAR. In addition to MWR data, this method assimilates JMA surface meteorological observations of temperature and water vapor and wind data from wind profilers. In the 1DVAR of this study, 48 vertical layers were calculated from the ground to an altitude of about 21 km, and the analysis variables were temperature, pseudo-relative humidity, and wind. The LBFGS method, which is also used for JMA mesoscale analysis, was applied for the minimum value search. The results of the JMA operational mesoscale model (MSM) were used as the first estimate (Guess), and the 1DVAR analysis was performed every 10 minutes in real time at all MWR stations.

To verify the accuracy of the 1DVAR, we compared it with the results of the July-August 2022 sonde observations at Naze (Fig. 3) when no rain was observed within 1 hour before and after sonde observations, since rain causes errors in MWR observations. The results showed that for temperature, the bias (mean difference: MD) and root-mean-square (RMS) difference were smaller for 1DVAR than for NN and Guess. For water vapor density, the MD and RMSE of 1DVAR were smaller than those of NN and Guess. This confirms that 1DVAR with MWR data can be used to obtain highly accurate temperature and water vapor profiles.

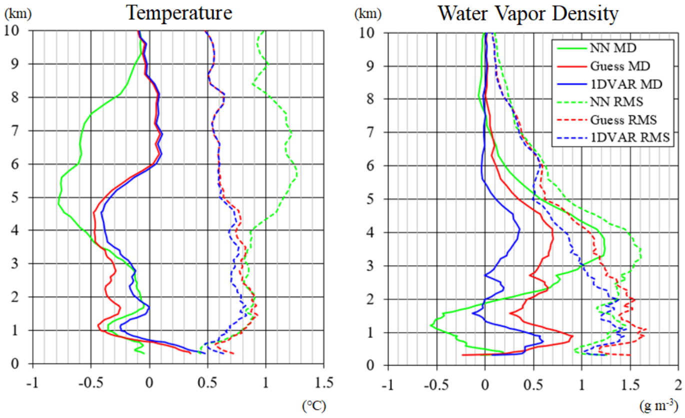

Figure 3. Accuracy of profiles for temperature and water vapor density, based on 1DVAR, first guess of MSM (Guess) and neural network (NN) profiles based on observations at Nase during July and August 2022. The bias (Mean Difference: MD, solid line) and variability (RMS, dashed line) of each profile with respect to the sonde observations are shown for temperature on the left and for water vapor density on the right. 100 cases without rain within 1 hour before or after the time of the sonde observation are used for verification.

4. Case study on monitoring atmospheric conditions

As the initial results of the MWR monitoring system, Fig. 4 shows the temporal changes in precipitable water vapor (PWV) and CAPE at Nase from July 5 to 11, 2022. Note that it is difficult to compare absolute values due to the different elevations of the MWR, sonde (Sonde), and model (Guess). The trends of PWV and CAPE obtained from Sonde, 1DVAR, and NN are in good agreement, and the variations in PWV and CAPE that cannot be expressed by Guess (e.g., 09-15 JST (= UTC+9h) on July 7, yellow arrow in Fig. 4) can be expressed by 1DVAR and NN. This result suggests that the MWR data captures abrupt changes in atmospheric conditions well.

On July 9, 2022, the MWR at Nase observed inflows to the developed precipitation system (orange arrow period in Fig. 4). Temporal variations of atmospheric conditions based on 1DVAR analysis are shown in Fig. 5. Precipitation was observed around 15 JST on 9, and the water vapor flux increased in the lower atmosphere below 1 km altitude until around this time. Correspondingly, the water vapor density in the lower atmosphere also increased, resulting in a rapid instability of the atmospheric conditions. After the precipitation, the water vapor density in the lower atmosphere increased, but the amount of precipitable water rapidly decreased due to the inflow of air with a low equivalent potential temperature (EPT) into the middle atmosphere.

From these results, the monitoring system using MWR data and the 1DVAR technique would be beneficial for real-time monitoring of atmospheric conditions in severe weather.

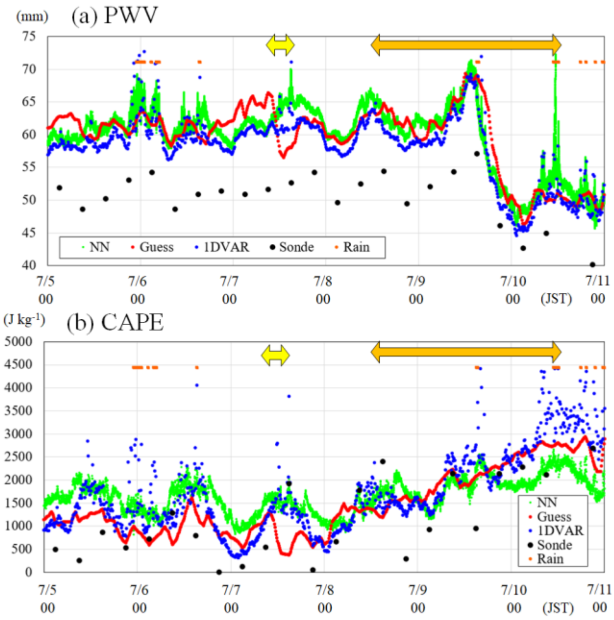

Figure 4. Time series of (a) precipitable water vapor (PWV) and (b) CAPE at Naze for July 5-11, 2022. Dots represent NN in green, Guess in red, 1DVAR in blue, and sonde observations in black. Orange dots mean rain. The elevations of the MWR and Sonde stations, and Guess are 3 m, 295 m, and 53 m, respectively.

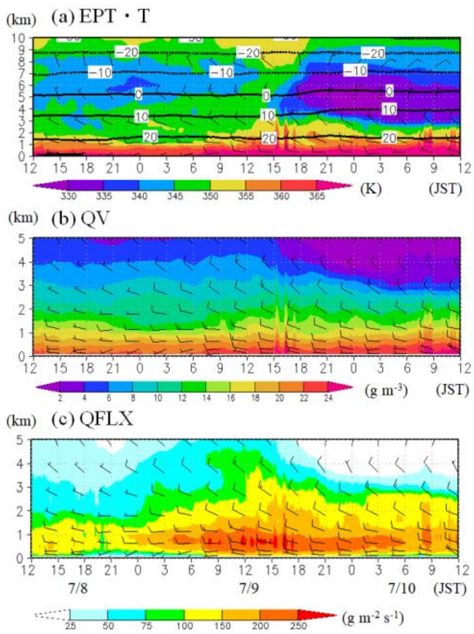

Figure 5. Time-height cross sections of the environmental field at Nase from 12 (JST) on 8 to 12 (JST) on 10 July 2022, obtained from 1DVAR analyses of (a) EPT (K, shaded) and temperature (°C, contours), (b) water vapor density (QV, g m^{-3}), and (c) water vapor flux (QFLX, g m^{-2} s^{-1}). Barbs indicate horizontal wind derived from 1DVAR analysis.

References:

Araki, K., M. Murakami, H. Ishimoto, and T. Tajiri, 2015: Ground-based microwave radiometer variational analysis during no-rain and rain conditions. *SOLA*, **11**, 108–112.